SAKARYA ÜNİVERSİTESİ
FEN BİLİMLERİ ENSTİTÜSÜ DERGİSİ

Sakarya University Journal of Science
SAUJS

e-ISSN: 2147-835X | Founded: 1997 | Period: Bimonthly | Publisher: Sakarya University
http://www.saujs.sakarya.edu.tr/en/

Title: Spatial Appraisal of Seasonal Water Yield of the Sokoto-Rima Basin

Authors: Saheed Adekunle RAJI, Shakirudeen ODUNUGA, Mayowa FASONA

Recieved: 2020-09-25 21:05:23

Accepted: 2021-06-21 14:51:17

Article Type: Research Article

Volume: 25
Issue: 4
Month: August
Year: 2021
Pages: 950-968

How to cite
Saheed Adekunle RAJI, Shakirudeen ODUNUGA, Mayowa FASONA; (2021), Spatial Appraisal of Seasonal Water Yield of the Sokoto-Rima Basin. Sakarya University Journal of Science, 25(4), 950-968, DOI: https://doi.org/10.16984/saufenbilder.800302
Access link
http://www.saujs.sakarya.edu.tr/en/pub/issue/64755/800302

Sakarya University Journal of Science 25(4), 950-968, 2021

Spatial Appraisal of Seasonal Water Yield of the Sokoto-Rima Basin

Saheed Adekunle RAJI*[1], Shakirudeen ODUNUGA[2], Mayowa FASONA[3]

Abstract

Understanding the dynamics of water yield related to water balance is vital for the functioning of ecosystems and model-based computation of their respective ecosystem services. This is important for valuable water resource planning and management in dryland regions, such as the Sokoto-Rima basin. In this study, we assess the spatiotemporal dynamics of quickflow (QF), local recharge (LR), and baseflow (B) between 1992 and 2015 with the use of the Seasonal Water Yield (SWY) model of InVEST (Integrated Valuation of Ecosystem Service and Tradeoffs) software. Pre-classified landcover, rainfall, satellite-derived evapotranspiration, digital surface topography, and HYSOGs 250m soil datasets were used as software input. The result of the study showed that QF, LR, and B depict similar spatial distribution with peak values generated within water-bearing landcover areas, particularly water bodies and wetlands. QF was highest in 2002 (1,293.6 mm), and the subsequent years – 2012 and 2015 had reductions. Similar patterns were observed in LR and B with much lower values. The temporal trend for the 23-year period of the study showed that QF had an increasing rate of 85.331 mm while decreasing rates of 56.131 mm and 27.597 mm were detected for LR and B, respectively. Three essential parameters – alpha (α), beta (β), and gamma (γ) showed evidence of sensitivity to changes in seasonal water yield values. These water balance transactions provided an opportunity to review the impact of the sensitivity of the landcover, climate, and hydrogeological factors on water resources management, mainly freshwater accounting in the Sokoto-Rima basin of the northwestern part of Nigeria.

Keywords: Quickflow, local recharge, baseflow, InVEST, ecosystem services.

1. INTRODUCTION

Ecosystem services are, in many ways more than one, connected to freshwater systems and, by extension, convolutedly linked to socioeconomic development and human welfare [1-3]. This is because of the inevitability of water for food, medicine, and other human consumptive purposes, industrial heating and cooling, irrigation and other agrarian purposes, habitat for different species, support wetland functioning, and assessment of environmental dynamics [1-5].

*Corresponding author: E-mail: raji.saheed@fupre.edu.ng
[1] Federal University of Petroleum Resources Effurun, Department of Environmental Management and Toxicology, Effurun, Nigeria.
ORCID: https://orcid.org/0000-0002-5890-5414.
[2] University of Lagos, Department of Geography, Akoka-Yaba, Lagos, Nigeria.
E-mail: sodunuga@unilag.edu.ng
ORCID: https://orcid.org/0000-0003-4307-9428.
3 University of Lagos, Department of Geography, Akoka-Yaba, Lagos, Nigeria.
E-mail: mfasona@unilag.edu.ng
ORCID: https://orcid.org/0000-0002-7876-7397.

One of the natural attributes that can be used to define freshwater ecosystem services is water yield [6-8]. Water yield defines the amount of water available in a particular area regarding provisioning and regulatory functions; consequently, it is correlated with land use dynamics [6-7]. This is why the quantitative assessment of water yield is a valuable tool for expressing the nexus between populace and water. In addition, quantitative assessment of water yield can help in effective surveillance and management of water resources, particularly in a well-defined hydrological basin, by tracking changes and ensuring sustainability [4,5-8]. Key environmental factors such as precipitation, evapotranspiration, soil-water interrelations, terrain configuration and geology, vegetation and land use dynamics are measured [6-8].

Combining these factors to estimate water yield can be laborious, especially in data-scarce jurisdictions where data on environmental monitoring and hydrologic changes are unavailable, and inconsistent collection approaches were accessible [6]. Models are often used to resolve these challenges in which the environmental factors formed the foundational model inputs [7]. However, the paucity of suitable data typologies and formats can render the anticipated assessment sought by the model implausible. Reliance on satellite data sources and those generated using spatial statistics have been utilised to provide spatial visualisations of water yield.

Since models are a systematic replica of the natural world, the uncertainty of parameters measured from their outputs is vital [6, 7]. As regards freshwater ecosystem services, model estimates are often defined based on water inputs and output pathways in consideration of localised environmental conditions. Analysis of these uncertainties of these parameters via sensitivity to changes will help measure place-specific quantification assessments to identify controlling factors and influence on water yield. Also, this performance assessment will provide a good rank of parameters connected to local processes and controls on water yield. Literature on the application of these measures within the semi-arid ecosystem of West Africa remains a rarity. Existing measures are often based on non-spatial hydrological assessments such as [8-10].

Even though Nigeria is moderately water rich with per capita annual water availability value of 1,158 m^3 [11], this is spatially restricted to the south with a high all-year-round water density. İn the north, including the Sokoto-Rima basin, optimal functioning of freshwater ecosystem service complexes remains seasonal hence the heavy reliance on dams and irrigation projects to supply urban and agrarian purposes. However, researches on water yield have often concentrated on annual water yield [8-10, 12-13], while a few, such as [6-7], considered the import of seasonal water yield. These studies have shown that seasonal water yield is sufficient to capture the value of seasonal differences in water resource management, particularly for irrigation management, water requirements for crops, and urban water supplies in arid zones. However, these latter studies showcased the essence of seasonal water yield for dryland hydrological settings such as the Sokoto-Rima basin, existing studies such as [8, 10] focussed on a fraction of the issue. Questions on the dynamics and influence of seasonal water fluctuations remain largely unanswered. Knowing this will help address localised water scarcity issues as seasonal water deficit within the semi-arid is largely place-based.

In this research, the InVEST (Integrated Valuation of Ecosystem Services and Tradeoffs) seasonal water yield (SWY) model was employed in the Sokoto-Rima basin of the northwestern axis of Nigeria. Three water yield outputs, namely quickflow, baseflow and local recharge, were computed spatiotemporally. Notably, the SWY model was created by the Natural Capital Project (www.naturalcapitalproject.stanford.edu) based on the water-balance concept [19]. Also, the sensitivity of the vital parameters was assessed. The study results are expected to apply to other semi-arid areas in northern Nigeria and West Africa at large.

2. MATERIAL AND METHODS

2.1. The Study Area

The Sokoto-Rima basin is a transnational hydrological basin of West Africa that covers Nigeria, Benin and Niger. Nevertheless, this section of the study falls within the Nigeria section, which swaths within Latitudes 10˚32'35" N to 13˚32'55" N and Longitudes 3˚30'30" E to 8˚1'15" E with a total land area of 94,026.50 km^2 (Figure 1). Based on climate, the mesoscale convective processes associated with the tropical savanna climate of West Africa [14] directly influenced the research area. Two highly distinguished climatic seasons - wet and dry subsists with clearly defined rainfall and temperature variations. Mean annual rainfall ranges from 350 mm to 895 mm from north to south, increasing the spatial index. Mean temperature annually averages 30 ^{0}C with substantial variability where the value increases during the wet and post-dry seasons and low during the dry season [15].

Rivers and streams that flow under the influence of relief and elevation characterized freshwater systems of the Sokoto-Rima basin. The critical river systems are the Sokoto and Rima, where the basin derives its name. It flows from westwards with a series of confluences with Rivers Zamfara, Ka, Bunsuru, Maradi, Gagere, Konni and others. The relief rises from the eastern basement complex rocks with an elevation of 802 m above sea level and reduced to the lowest around the Niger plain south of the study area. The surrounding wetlands and plains have been subjected to extensive cultivation defining the agrarian nature of the Sokoto-Rima basin. Water-sensitive crops such as rice, millet, sorghum, maize have been cultivated with cattle, ram, sheep and goat domestically reared.

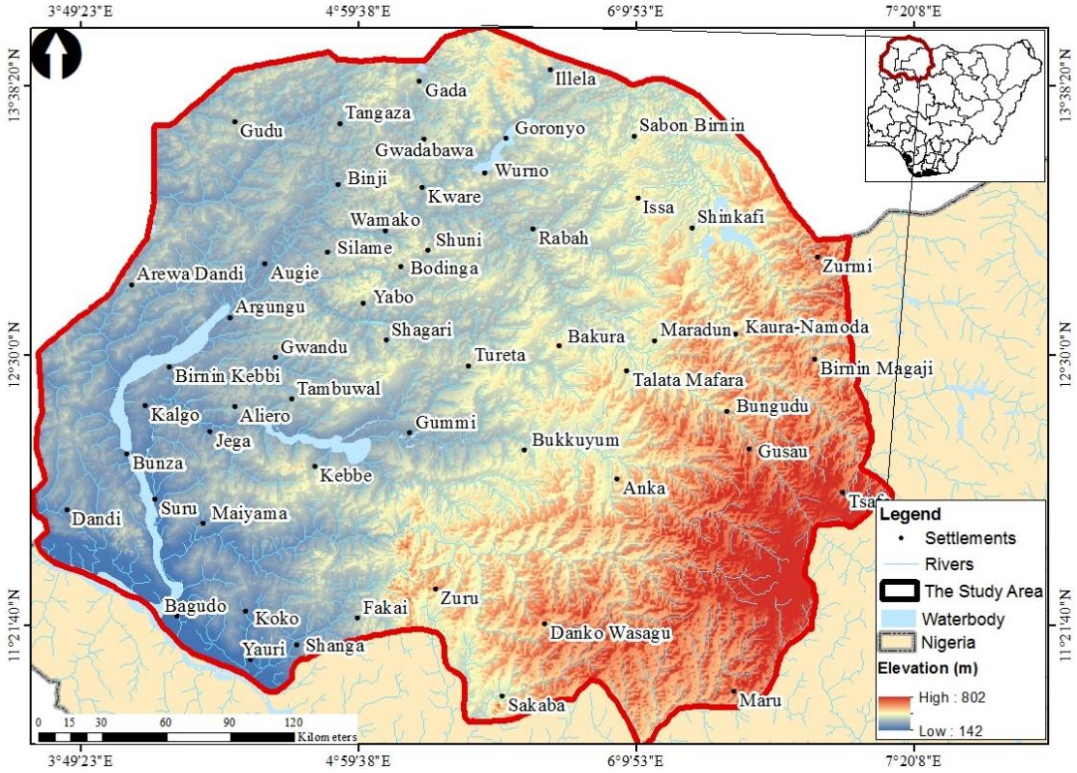

Figure 1 Location of the Sokoto-Rima basin in context of northern Nigeria with relief and the network of rivers and streams defining the basin

2.2. Data Sources and Characteristics

Multi-sourced spatial data with unique characteristics were used in this study. As shown in Table 1, we sourced these datasets from various archives and existed as texts, tables, raster and vector data files. So, to avoid computational incompatibilities, all the datasets were converted

using Geographical Information Systems (GIS) software to raster datasets, re-sampled to 100 metres spatial resolution and projected to Universal Transverse Mercator Zone 31 North (UTM Zone 31 N), where the study area is located. The associated data sources and other details are concisely presented in Table 1.

Table 1 Data characteristics and sources used in this study

s/N	Data	Resolution	Year	Data Source
1	CCI-LC Climate Change Initiative Landcover	300 metres	1992 2002 2012 2015	European Space Agency (ESA) Climate Change Initiative (CCI) Data Viewer at http://maps.elie.ucl.ac.be/CCI/viewer/profiles.php
2	Evapotranspiration (Eta version 4) v4 data	250 metres	1992 2002 2012 2015	USGS Famine Early Warning System (FEWS) Data for West Africa https://earlywarning.usgs.gov/fews/product/451
3	TAMSAT	0.0375° (~ 4 km)	1983-2019	Tropical Applications of Meteorology using Satellite data and ground-based observations https://www.tamsat.org.uk
4	Shuttle Radar Topography Mission (SRTM) 4.1	90 metres; vertical accuracy of 16 metres	2014	CGIAR Consortium for Spatial Information https://srtm.csi.cgiar.org/
5	HYSOG Soil Group	250 metres	2015	United States Oak Ridge National Library Distributed Active Archive Centre (ORNL DAAC) https://daac.ornl.gov/cgi-bin/dsviewer.pl?ds_id=1566
6	eMODIS NDVI Data	250 metres	2002 2012 2015	USGS Famine Early Warning System (FEWS) Data for West Africa https://earlywarning.usgs.gov/fews/product/451
7	Curve number (CN)	Dimensionless with range (0-100)	2007	Handbook of the United States Department of Agriculture (USDA) accessed online at https://directives.sc.egov.usda.gov/OpenNonWebContent.aspx?content=22526.wba
8	Crop/vegetation coefficient (Kc)	Dimensionless with range (0.114–0.689)	1998	Monthly crop factor values generated from the archives of the Food and Agriculture Organization of the United Nations (FAO) available online at the webportal: http://www.fao.org/3/x0490e/x0490e00.htm

The pre-classified and pre-processed Climate Change Initiative (CCI) landcover data of the European Space Agency (ESA) was used as the central data spine of the study. It has a spatial resolution of 300 meters and a 32-bit quantisation level sufficient to detect homogenous landcover classes. Its pre-processed nature ensures that edge-matching errors constraining large-scale utility have been eliminated. The period 1992, 2002, 2012 and 2015 were acquired based on data available from the data download portal http://maps.elie.ucl.ac.be/CCI/viewer/profiles.php.

Satellite-derived actual evapotranspiration (ETa) data for the periods 1992, 2002, 2012 and 2015 were sourced from the portal of the United States Geological Survey (USGS) Famine Early Warning Systems Network (FEWSNET) and produced using the Moderate Resolution Imaging Spectroradiometer (MODIS). The datasets were generated through the operational simplified surface energy balance (SSEBop) model advanced by [16] with a spatial resolution of 250 metres.

Also, rainfall datasets were generated from the Tropical Applications of Meteorology using Satellite data and ground-based observations (TAMSAT) specifically for Africa. The data was sourced from https://www.tamsat.org.uk/. It has a medium resolution of 0.0375° (roughly 4 km), suitable for defining long-term tropical climatology, particularly from a monsoon region. The acquired data was presented in netCDF format, which is suitable for GIS-based

application. Further details of satellite characterisation and ex-situ processing of TAMSAT data are available in [17].

Digital surface topography data was sourced from the Shuttle Radar Topography Mission (SRTM), having 90-metre (3-arc-second) spatial resolution. The data was acquired from the CGIAR Consortium for Spatial Information (CGIAR-CSI). It has a minimum vertical accuracy of 16 m which is suitable for the study.

Global Hydrologic Soil Groups (HYSOGs250m) data sourced from NASA's Distributed Active Archive Centre for Biogeochemical Analysis (DAAC) data employed in the study was via https://daac.ornl.gov/SOILS/guides/Global_Hydrologic_Soil_Group.html. İt has a spatial resolution of 0.002083° (250 m). The data is vital for ecohydrological modelling at a regional scale [18].

Other datasets acquired for the study include landcover sensitive CN (curve number), a pragmatic variable used to estimate direct hydrologic runoff or infiltration from excess precipitation. The values used in this study were extracted from the handbook of the United States Department of Agriculture (USDA). The monthly crop/vegetation coefficient (Kc) values for different landcover typologies within a cultivated semi-arid zone of the tropics were referenced from the archives of the Food and Agriculture Organization Food and Agriculture Organization of the United Nations (FAO).

2.3. Description of the InVEST Seasonal Water Yield (SWY) Model

Spatially explicit models are essential for estimating hydrological patterns, particularly in areas characterised by low and inconsistent data availability. These models are often used to augment data gaps for spatial planning of water ecosystem services and related resource management. This study adopted the InVEST SWY model because of its low data requirements, inherent spatially explicit nature of depicting water routing, and adoption of a streamlined water balancing approach [19]. The latter, however, has some level of uncertainty whose influence on water appraisal ability must be determined.

A comprehensive description of the InVEST SWY model can be found in [19]. The main computational procedure and the essential variables thereof are presented in this study, as shown in Figure 1. Four segmentation levels can be identified in the model. First, it computes quickflow (QF) at the interannual (monthly) level per pixel of the multispectral space. This is based on the NRCS curve number method, which calculates approximately interannual direct runoff using monthly precipitation and the number of rain events per period [28]-[34]. This is defined as:

$$QF_{i,m} = n_m \left(\left(a_{i,m} - S_i\right) exp\left(-\frac{0.2S_i}{a_{i,m}}\right) + \frac{S_i^2}{a_{i,m}} exp\left(\frac{0.8S_i}{a_{i,m}}\right) E_1\left(\frac{S_i}{a_{i,m}}\right)\right) (25.4\left[\frac{mm}{in}\right]) \quad (1)$$

$$QF_i = \sum_{m=1}^{12} QF_{i,m} \quad (2)$$

where: S_i latent highest soil moisture holding sequel to water flow; C_{NI} is the curve number for pixel *i*; $a_{i,\,m}$ is the mean rain depth on a rainy day at pixel *i* on month *m*; E_1 is the change integral function; and *t* is study period.

Second, the model segregates monthly available water between local recharge and evapotranspiration. On a particular pixel, this division is affected by factors that influence the availability of subsurface water for evapotranspiration, namely by up-slope recharge and α, β and γ parameters. Thus, evapotranspiration is defined as:

$$AET_{i,m} = \min\left(PET_{i,m}; P_{i,m} - QF_{i,m} + \alpha_m \beta L_{sum.avail,i}\right) \quad (3)$$

where $L_{sum.avail,i}$ is the sum of upslope subsurface water that is hypothetically accessible at pixel *i*, β is a spatial accessibility parameter that ranges between 0–1 and influenced by local terrain characteristics, and α_m is the portion of the (annual) upslope water support that is accessible in a given month *m*. The γ parameter, though optional, is a defined as a function of recharge at

a given pixel level within the multispectral space that is accessible and not lost to pixels at the downslope level. Third, the model computes the local recharge (LR) on a given pixel, which denotes the probable subsidy to aggregate annual baseflow:

$$L_i = P_i - QF_i - AET_i \quad (4)$$

where: L_i is the index of LR P_i annual precipitation of pixel i, QF is the yearly quickflow, AET_i actual evapotranspiration aggregated from monthly levels. Finally, index of Baseflow (B), i.e. the amount of water that gets to the stream, is computed as:

$$B_i = B_{sum,i} * \frac{L_{avail,i}}{L_{sum,}} \quad (5)$$

given that: $L_{sum,i} = L_i + \sum_j^i L_{sum,j} * P_{ji}$ (6)

where B_i is baseflow of pixel i, $L_{sum,i}$ is cummulative upstream recharge of pixel i.

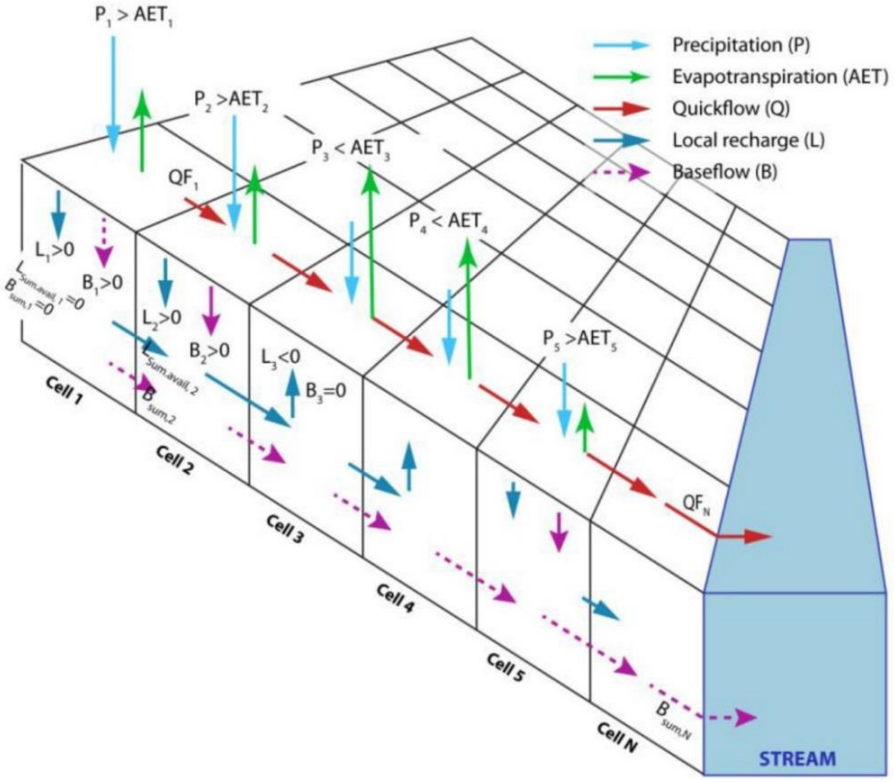

Figure 2 The InVEST Seasonal Water Yield model hydrologic channelling system depicting the pixel-based one-dimensional water flow path primed upon the simplified water balance approach (Source: [7])

2.4. Sensitivity Analysis of the InVEST SWY Model

The sensitivity of the critical variables of the SWY model was tested singularly as a measure of model performance and robustness. This analysis also provides an opportunity for testing the flexibility of the vital model-defining parameters per pixel within the multispectral space. The tested parameters were coefficients embedded in the model as provided by [19]. Notably, the variation of α showcases the import of interannual precipitation changes coupled with the possible unchanged local regime for a semi-arid area where water recharge is essential for different uses. Also, β is influenced by terrain characteristics, specifically soil typology and geology; hence, it is often less dynamic. Storage capacity, up-slope subsidy, and up-slope area are essential considerations when setting the numerical influence of β within the model. g parameter is also terrain influenced as observed with β but more on edaphic controls such that level of permeability often affects seasonally available water within a region. Due to the large-scale uniformity of soil-water context, the g parameter is often unchanged over the landscape. V parameter is the number of up-slope pixels that

contribute to a stream's definition in a given pixel. As a result, V is a function of SRTM data, and improvement in resolution characteristics could influence the expression of stream pixels within the multispectral space. V, α, β, and g parameters were adjusted by ±50% due to the possible nature of water fluctuation in a typical semi-arid region where there is established interannual water fluctuation. Expressly, V was varied from the default value of 1,000 to 500 and 1,500. The α parameter was also adjusted from the default value of 1/12 (indicating annual fluctuation) to 1/6 (biannual) and 1/24 (biennial). At the same time, both β and g were varied from the default value of 1 to ½ and 1½ each.

3. RESULT AND DISCUSSION

3.1. Spatiotemporal Dynamics of Quickflow in the Sokoto-Rima basin

The spatial distribution of quickflow, which is the hydrological response to direct water input from rainfall leading to increase river runoff within short intervals, is depicted in Figure 3. At the same time, the status levels were presented in Table 2. Five status levels were detected throughout the study periods, with fluctuating maximum and minimum values. This is not uncommon as quickflow characterisation is never highly dynamic [29]. However, the quickflow of the Sokoto-Rima basin is dominated by low flow levels with very low and low statuses. For instance, in 1992, the very low flow status occupied 38.15% (35,868.32 km^2) by the year 2015, it falls to 28.17% (26,490.24 km^2), while very high flow status improved from 9.07% (8,529.15 km^2) to 11.65% (10,950.54 km^2) suggesting that more areas received post-rainfall flow within 23 years. Also, the pattern of the shift in the amount of quickflow though disproportionate, shows increases over the years. Specifically, 38.5% increase in the low flow and a 19.63% upsurge in the magnitude of high flow. The associated temporal trend as displayed in Figure 6 portrays an increasing magnitude of quickflow with increasing rate of 85.331 mm per pixel with a pixel-based mean of 858.128 mm within the study period.

These intermittently high values of quickflow were spatially restricted to the headwaters located in the eastern part of the Sokoto-Rima basin (Figure 3). From these headwaters, quickflow was distributed spatially to other parts of the Sokoto-Rima basin. High quickflow values were also detected at the wetlands areas of the southern axis. The high quickflow observed within the downstream is partly due to its inherent landcover as mainly extensive wetlands of the Niger plain. As shown in Figure 3, the spatial pattern of quickflow distribution showed diverse values for each study period (a function of rainfall and other environmental factors). As shown in Figure 3, there is a south-north decreasing pattern of quickflow with exceptions in water-bearing landcover themes such as rivers, streams, lakes and dams in locations such as Sokoto, Goronyo, Talata-Mafara, Yauri, Maradi Argungu and Gusau, amongst others.

Table 2 Quickflow dynamics and relations in the Sokoto-Rima basin

1992			2002			2012			2015		
Status/ Modelled QF (mm)	**Land area (km^2)**	**%**	**Status/ Modelled QF**	**Land area (km^2)**	**%**	**Status/ Modelled QF**	**Land area (km^2)**	**%**	**Status/ Modelled QF**	**Land area (km^2)**	**%**
Very low (0-98.97)	35,868.32	38.15	Very low (0-151.11)	26,338.26	28.01	Very low (0-130.86)	30,607.87	32.55	Very low (0-137.07)	26,490.24	28.17
Low (98.98-267.06)	20,182.86	21.47	Low (151.12-411.23)	28,229.01	30.02	Low (130.87-363.79)	24,471.20	26.03	Low (137.08-385.93)	29,565.14	31.44
Moderate (267.07-453.42)	16,589.86	17.64	Moderate (411.24-671.35)	15,372.18	16.35	Moderate (363.80-596.72)	16,716.83	17.78	Moderate (385.93-617.32)	13,462.24	14.32
High	12,856.32	13.67	High	15,370.37	16.35	High	14,177.96	15.08	High	13,558.34	14.42

(453.43-643.43)			(671.35-905.97)			(596.73-805.89)			(617.32-796.32)		
Very high (643.44-924.8)	8,529.15	9.07	Very high (905.98-1293.6)	8,716.68	9.27	Very high (805.90-1205.2)	8,052.64	8.56	Very high (796.33-1106.3)	10,950.54	11.65
Total	**94,026.5**	**100**	**Total**	**94,026.5**	**100**	**Total**	**94,026.5**	**100**	**Total**	**94,026.5**	**100**

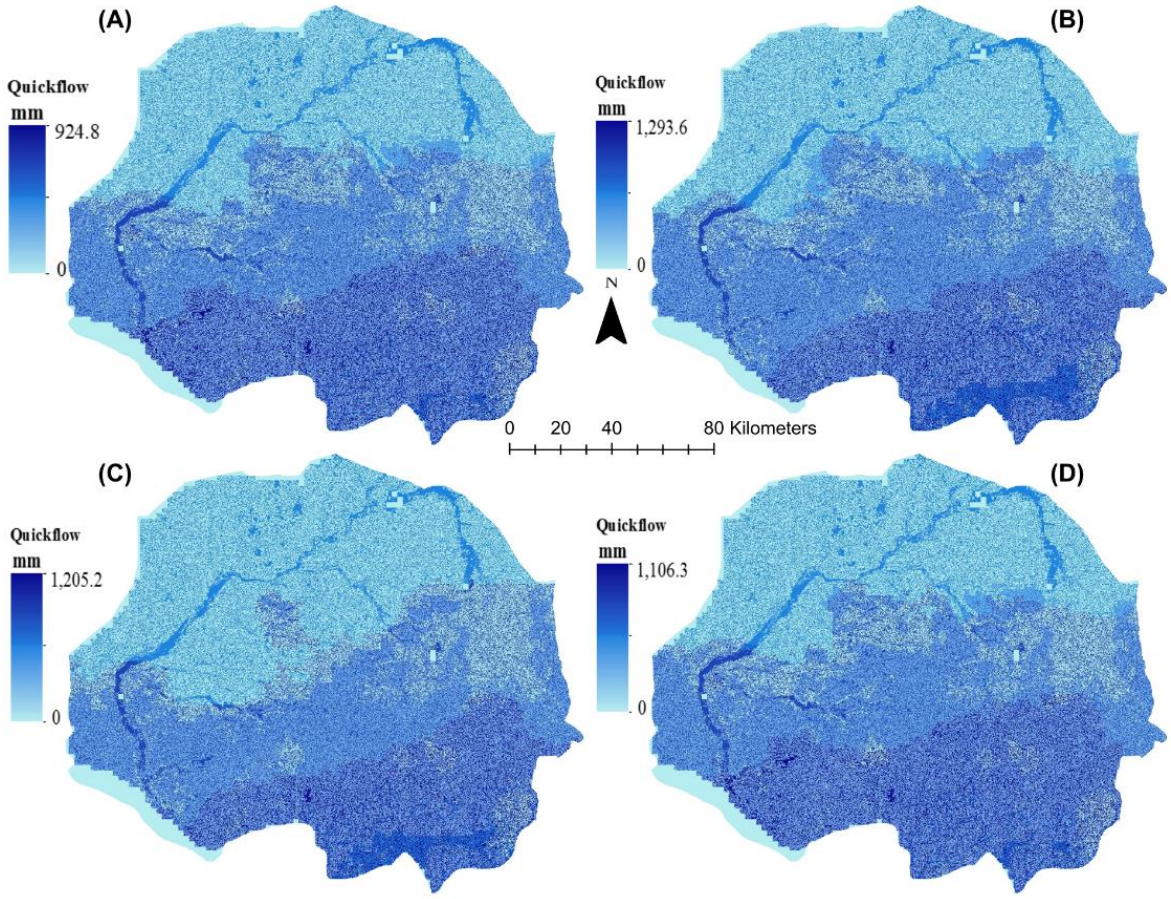

Figure 3 Spatial dynamics of quickflow of the Sokoto Rima basin for the year 1992 (A), 2002 (B), 2012 (C) and 2015 (D)

The spatial perspective of quickflow of the Sokoto-Rima basin for the study typified specifics that affirm the geography of post-floodwater distribution in the area. as displayed in Figure 4, the period 1992–2002 placed the marker for north-south change such that increases were detected in most parts of the south while decrease in quickflow was seen in the north. However, some areas of the west returned unchanged. The pattern changed significantly for the period 2002-2012: sustained increases were detected in some parts of the north that previously recorded decreases; similar patterns were also detected along the Sokoto River, particularly in parts of Kebbi; and a mosaic of decrease and unchanged patterns was detected in other parts of the study area. The period 2012-2015 showed the expansion of unchanged pattern, the dominance of declines in the east and increases in the west. On the whole, quickflow decreased northwards for the entire period of study, with local exceptions in some areas with specific socio-environmental influences.

These observations are not unexpected in dryland where rainfall drives hydrological response such that ephemeral streams become active and flash floods occur [9, 14-15]. Several factors have alluded to this. For instance, [8] asserted that water yield is a function of a consistent increase

in the amount of rainfall received per time in the Sokoto-Rima basin. [29] stated that apart from precipitation dynamics, landcover, change in vegetation could affect water yield, out of which quickflow is significant. [29] further affirmed that quickflow in low rainfall grassland area of Tibet contributes roughly 5% to water yield.

The contribution of quickflow in the expression of water yield remains critical, especially for semi-arid zones and for data-sparse regions where water availability data remain a daunting challenge [33, 31-33]. Quickflow is directly proportional to the amount of rainfall and landcover typologies. As a result, quickflow is a crucial factor in defining hydrological ecosystem services of the Sokoto-Rima basin. Quickflow is a vital index that aids water management for food security by boosting agriculture and ensuring energy security [33]. Therefore, consistent assessment of quickflow as a component of water yield is inevitable for the sustenance livelihoods and ecosystem services of the Sokoto-Rima basin.

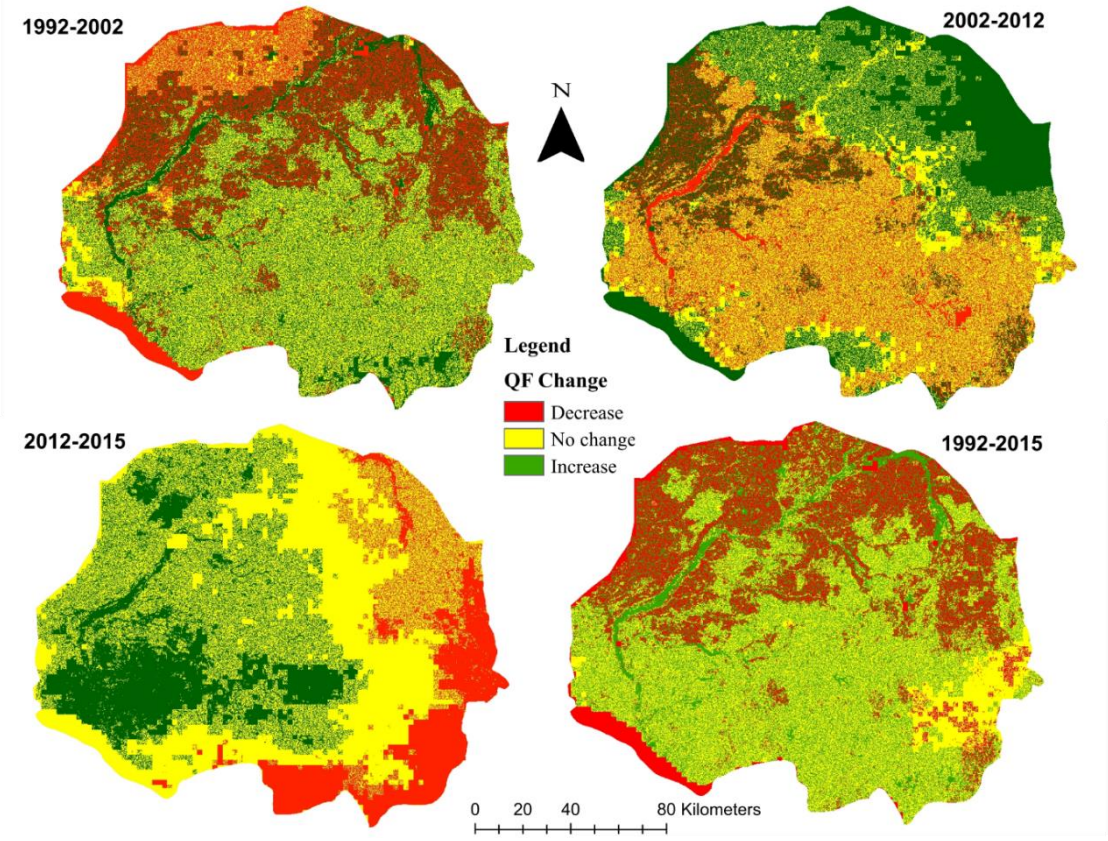

Figure 4 Pattern of spatiotemporal change in quickflow (QF) in the Sokoto Rima basin for the period 1992 to 2015

3.2. Spatial Variation of Local Recharge

As conceptualised in this study, variations in local recharge explain the pattern of changes in the potential contribution of rainfall (per pixel) in the basin to baseflow as influenced by the regional water balance. This shows that local recharge is directly proportional to excess rainfall feeding the groundwater and a significant factor in groundwater flow and characterisation. The spatiotemporal distribution of local recharge of the Sokoto-Rima basin for the study period is depicted in Figure 5, while the range of detected status is presented in Table 3. The concomitant temporal trend 6 portrays a decreasing magnitude of local recharge with rate of 56,131 mm per pixel with a pixel-based mean of 210,198 mm from 1992 to 2015 (Figure 6).

As shown in Table 3, local recharge is substantially low, averaging 46% very low status throughout the study. The very high grade recorded a meagre average of 0.025%, indicating a consistently low proportion and area extent. Overall, 71% of the low status were recorded

through strengthening the fact that the Sokoto-Rima basin is characterised by the low amount of water available per pixel. As depicted in Figure 5, the spatial equivalence of this shows that the south-north increasing index detected for the quickflow also subsists, though with periodic differentiations. Precisely, areas with a high amount of local recharge correlate directly with the extensive Niger plains. At the same time, moderate values were spatially delimited to some wetland areas while some of the permanent rivers and streams recorded the least importance. This scenario was detected in the baseline year (1992). By 2002, some wetlands in parts of the Sokoto-Shuni axis of the north recorded high values ranging from 311 to 931 mm, indicating an increase over time. This further expanded in 2012 to some parts of the headwaters of the northeast and the floodplains of the south. The trend persists till 2015, where roughly 13% of the landscape recorded a low amount of local recharge. The cumulative impact of the spatial distribution high amount of local recharge will lead to hydrological enrichment of the Sokoto-Rima basin, particularly wetlands and floodplains.

Table 3 Dynamics of Local Recharge characterisation in the Sokoto-Rima basin

1992			**2002**			**2012**			**2015**		
Status/ Modelled LR (mm)	**Land area (km^2)**	**%**	**Status/ Modelled LR (mm)**	**Land area (km^2)**	**%**	**Status/ Modelled LR (mm)**	**Land area (km^2)**	**%**	**Status/ Modelled LR (mm)**	**Land area (km^2)**	**%**
Very low (0-12.98)	45,611.11	48.51	Very low (0-61.29)	41,825.41	44.48	Very low (0-39.04)	41,883.66	44.54	Very low (0-44.74)	41,867.93	44.53
Low (12.99-82.54)	27,339.87	29.08	Low (61.3-180.02)	20,726.95	22.04	Low (39.05-141.66)	20,887.66	22.21	Low (44.75-143.96)	15,632.56	16.63
Moderate (82.55-169.48)	17,703.36	18.83	Moderate (180.03-311.94)	24,723.36	26.29	Moderate (141.67-257.11)	23,453.13	24.94	Moderate (143.97-243.18)	25,166.36	26.77
High (169.49-604.19)	3,347.04	3.56	High (311.95-931.98)	6,730.91	7.16	High (257.12-872.84)	7,781.82	8.28	High (243.19-725.11)	11,329.21	12.05
Very high (604.20-2273.5)	25.12	0.03	Very high (931.99-2620.6)	19.87	0.02	Very high (872.85-2527.6)	20.22	0.02	Very high (725.12-2567.8)	30.44	0.03
Total	**94,026.5**	**100**	**Total**	**94,026.5**	**100**	**Total**	**94,026.5**	**100**	**Total**	**94,026.5**	**100**

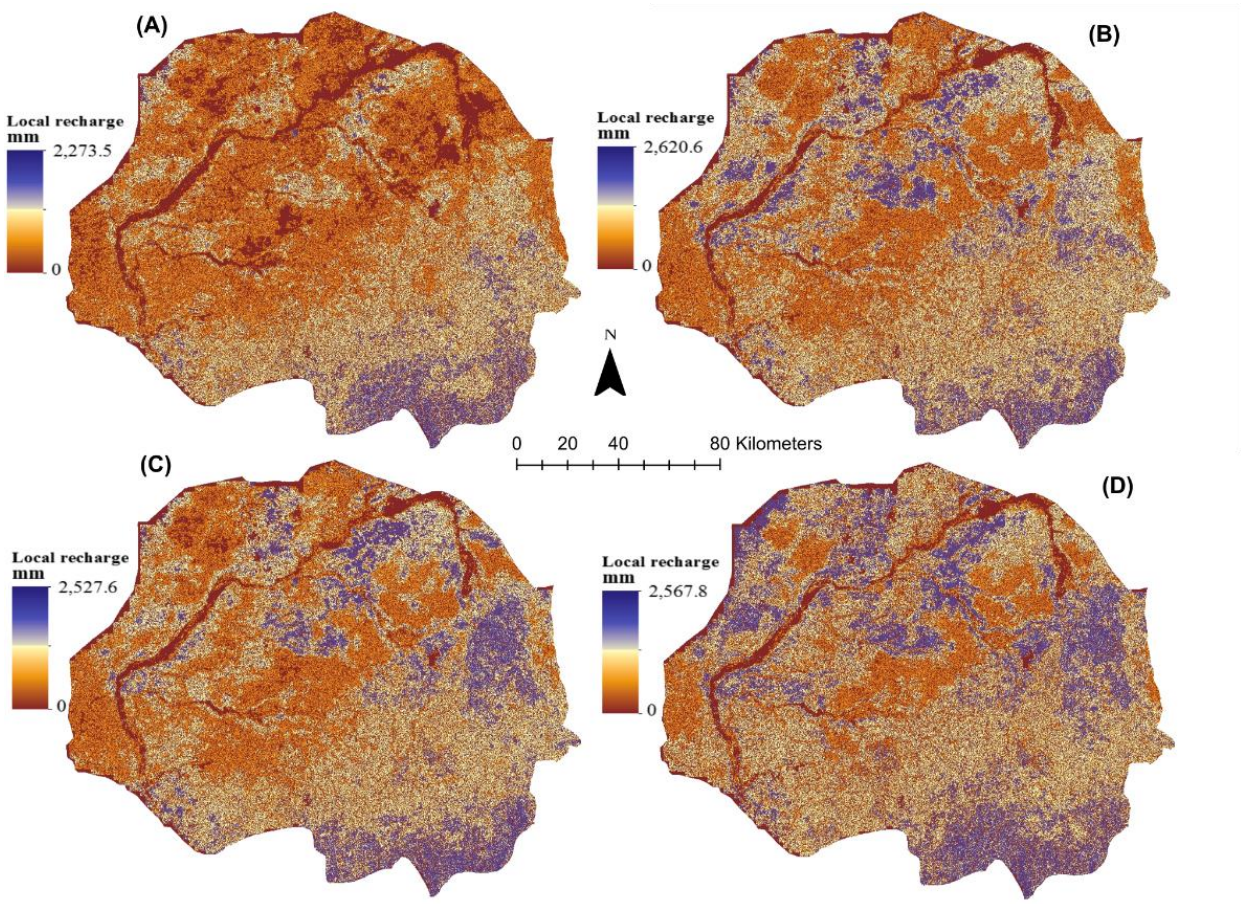

Figure 5 Spatial dynamics of local recharge of the Sokoto Rima basin for the years 1992 (A), 2002 (B), 2012 (C) and 2015 (D)

Relative to water balance, the amount of local recharge represents 2.5%, 5.1%, 2.6 and 2.3% of rainfall for 1992, 2002, 2012 and 2015, respectively. These are in concordance with [22], which computed that recharge rates for the Sokoto-Rima basin range between 2-7% of annual precipitation. It should be noted that hydrogeological factors influence the local recharge of a tropical basin such as the Sokoto-Rima. [23] affirmed that spatial distribution of artesian aquifers in locations such as Gundumi, Rima and Gwandu with varying depths influence available recharge. This is also to a great extent, geological age and associated constituents such as lithology, nature of deposits, and age range from the Cretaceous to Eocene. However, these aquifers are extensively confined apart from the open water bodies whose storage capacities with apparent seasonal climatic variations.

Marked distinctions exist within the spatial variations in local recharge of the Sokoto-Rima basin, as shown in Figure 7. This is obviously an accumulated characterisation of the observed spatiotemporal dynamics in local recharge relations and factors of change. The period 1992-2002 showed that wetland areas abutting the major rivers and streams recorded mixed increase and no change patterns throughout the study area. Decreases, however, were recorded in major rivers such as Sokoto, Rima, Ka, Maradi, and Zamfara. However, these observations flipped by the decade 2002-2012, where the increase was detected along with the water bodies, indicating ceteris paribus substantial water input. Minute instances of unchanged local recharge amounts were also detected all over the Sokoto-Rima basin. The period 2012-2015 witnessed few decreases and increase with no change dimension. For the entire study period, the magnitude of local recharge remained largely a mosaic of decrease interspersed with no change.

As shown in this study, local recharge (the proportion of local water balance that potentially feeds the baseflow) is a function of landcover,

precipitation and terrain characteristics. The result of the study also tallies with those of semi-arid areas of Ethiopia, particularly the Wabe Catchment of East Africa, with a similar spatiotemporal trend [32].

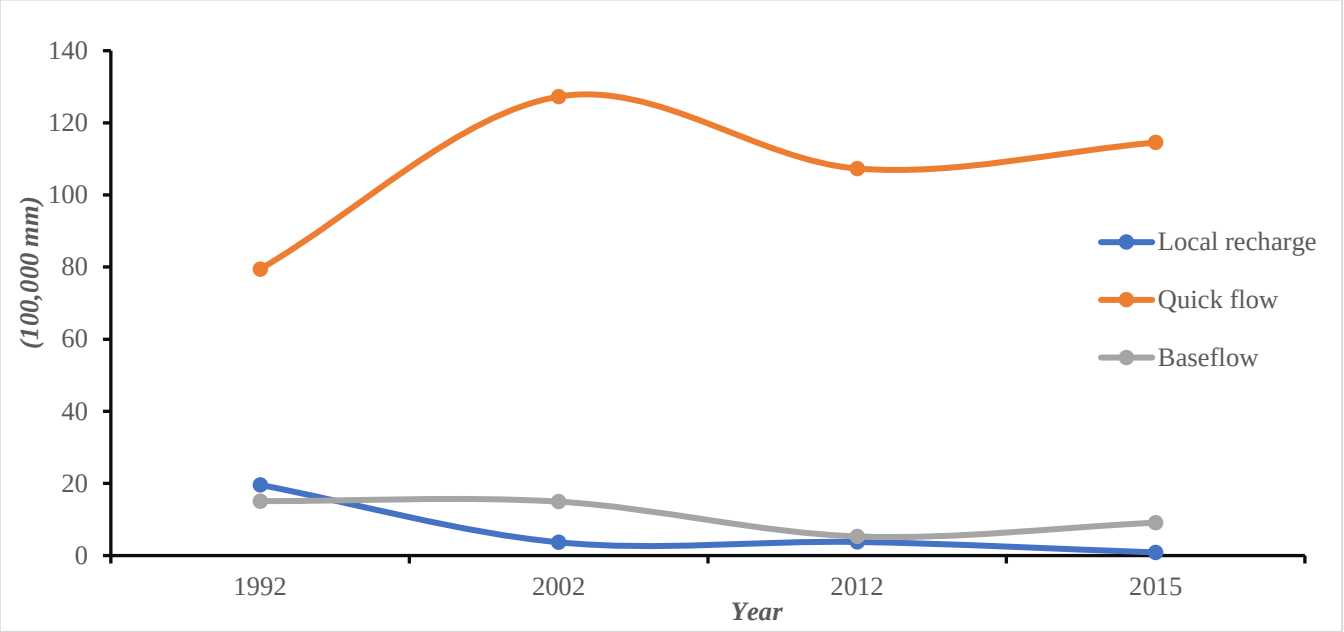

Figure 6 Temporal trend of quick flow, local recharge, and baseflow of the Sokoto-Rima basin for the period 1992, 2002, 2012 and 2015.

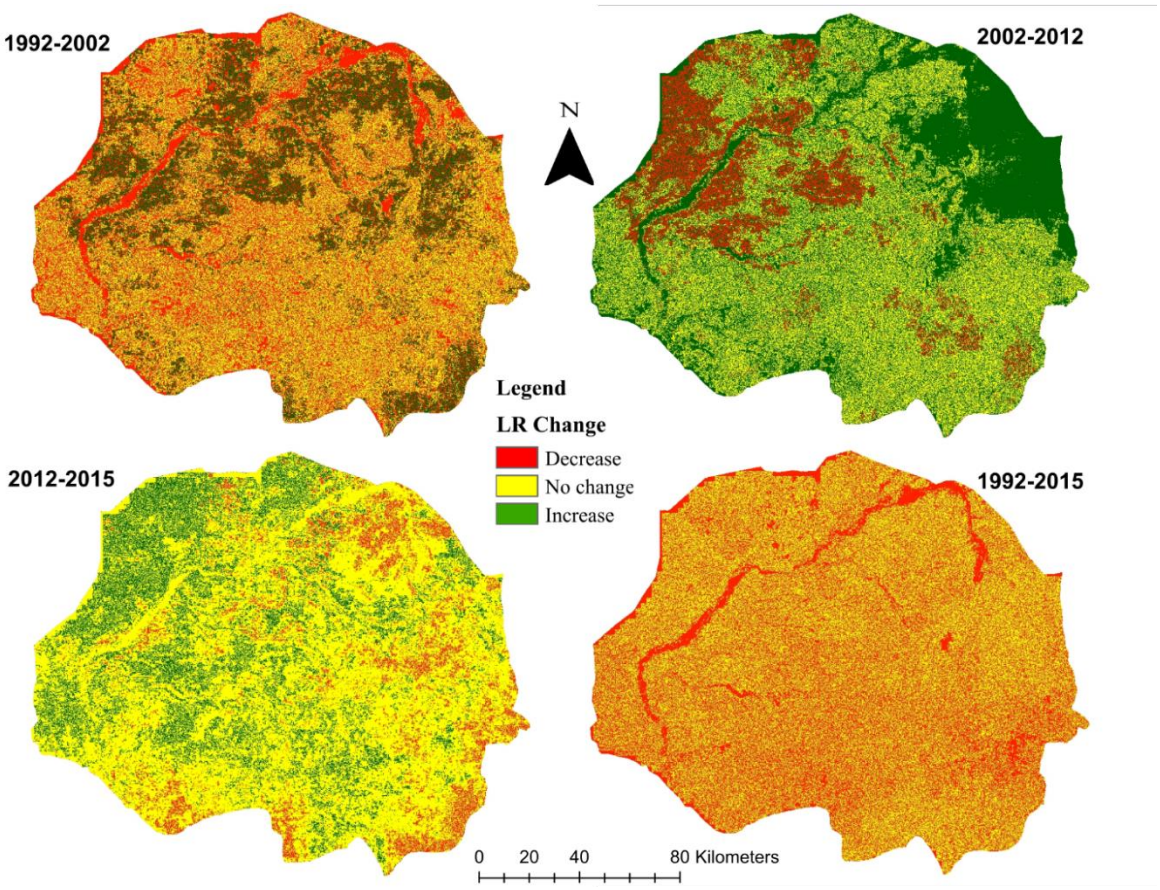

Figure 7 Pattern of spatiotemporal change in local recharge (LR) in the Sokoto Rima basin for the period 1992 to 2015

3.3. Baseflow Characteristics in the Sokoto-Rima

As developed in this study, Pixel-based baseflow is the actual contribution of a defined location in multispectral space to the amount of water that reaches a stream or a river [7, 19]. This shows that the equation of seasonal water yield is incomplete without the quantitative expression of baseflow. Spatial dynamics of baseflow in the Sokoto-Rima basin within the study period are presented in Table 4 and illustrated in Figure 8. Approximately 50% of the land area returned low baseflow status throughout the study period, while the proportion of high flow is <5% apart from 2002, which returned 5.4%. However, the proportion of moderate status has progressively increased from 18.27% (17,276.06 km^2) in 1991 to 26.28% (24,710.46 km^2) in 2015.

The associated spatial details revealed that the maximum baseflow level in 1992 was 4,723.43 mm; by 2002, it increased to 7.127.96 mm by a proportion of 50.91%. As shown in Figure 8, this change is primarily noticeable around water bodies and wetlands with substantial proportionate increases. The pattern observed in 2012 and 2015, as observed in Figure 8C and Figure 8D, showed a maximum of 6,771.24 mm and 5,888.58 mm, respectively depicting a gradual reduction by 5% and 17.39% from 2002 levels. Thus, the peak baseflow level of 7,127.96 mm was recorded in 2002. Decadal differences from 2002 to 2012 with reductions in the amount of baseflow, however, set regional delineations as decreases were recorded in the western part compared to increases in the west of and some parts of the northern section Sokoto-Rima basin. The temporal trend of baseflow in the Sokoto-Rima basin is shown in Figure 6 with decreasing pattern. Specifically, the trend showed a decreasing rate of 27.597 mm with an average yearly value of 180.189 mm within the period of study.

This correlates with the observation of quickflow and local recharge dynamics, particularly in locations where increases were detected. The further reductions noted in 2015 compared to 2012 mainly were detected in a few places in the east, while most of the study witnessed averagely unchanged values. The aggregate changes from 1992 to 2015 returned meagre changes over most of the Sokoto-Rima basin, while reductions in baseflow were observed in the north while wetlands of the central area had a tiny increase.

Table 4 Dynamics of Baseflow characterisation in the Sokoto-Rima basin

1992			**2002**			**2012**			**2015**		
Status/ Modelled B (mm)	**Land area (km^2)**	**%**	**Status/ Modelled B (mm)**	**Land area (km^2)**	**%**	**Status/ Modelled B (mm)**	**Land area (km^2)**	**%**	**Status/ Modelled B (mm)**	**Land area (km^2)**	**%**
Very low (0-98.97)	49,925.61	53.10	Very low (0-151.11)	39,967.39	42.51	Very low (0-130.86)	42,568.89	45.27	Very low (0-137.07)	39,495.79	42.00
Low (98.98-267.06)	24,475.97	26.03	Low (151.12-411.23)	28,242.14	30.04	Low (130.87-363.79)	28,100.93	29.89	Low (137.08-385.93)	25,342.58	26.95
Moderate (267.07-453.42)	17,276.06	18.37	Moderate (411.24-671.35)	20,067.47	21.34	Moderate (363.80-596.72)	19,684.30	20.93	Moderate (385.93-617.32)	24,710.46	26.28
High (453.43-643.43)	2,330.84	2.48	High (671.35-905.97)	5,074.19	5.40	High (596.73-805.89)	3,654.51	3.89	High (617.32-796.32)	4,396.64	4.68
Very high (643.44-924.8)	18.02	0.02	Very high (905.98-1293.6)	675.30	0.72	Very high (805.90-1205.2)	17.88	0.02	Very high (796.33-1106.3)	81.03	0.09
Total	**94,026.5**	**100**	**Total**	**94,026.5**	**100**	**Total**	**94,026.5**	**100**	**Total**	**94,026.5**	**100**

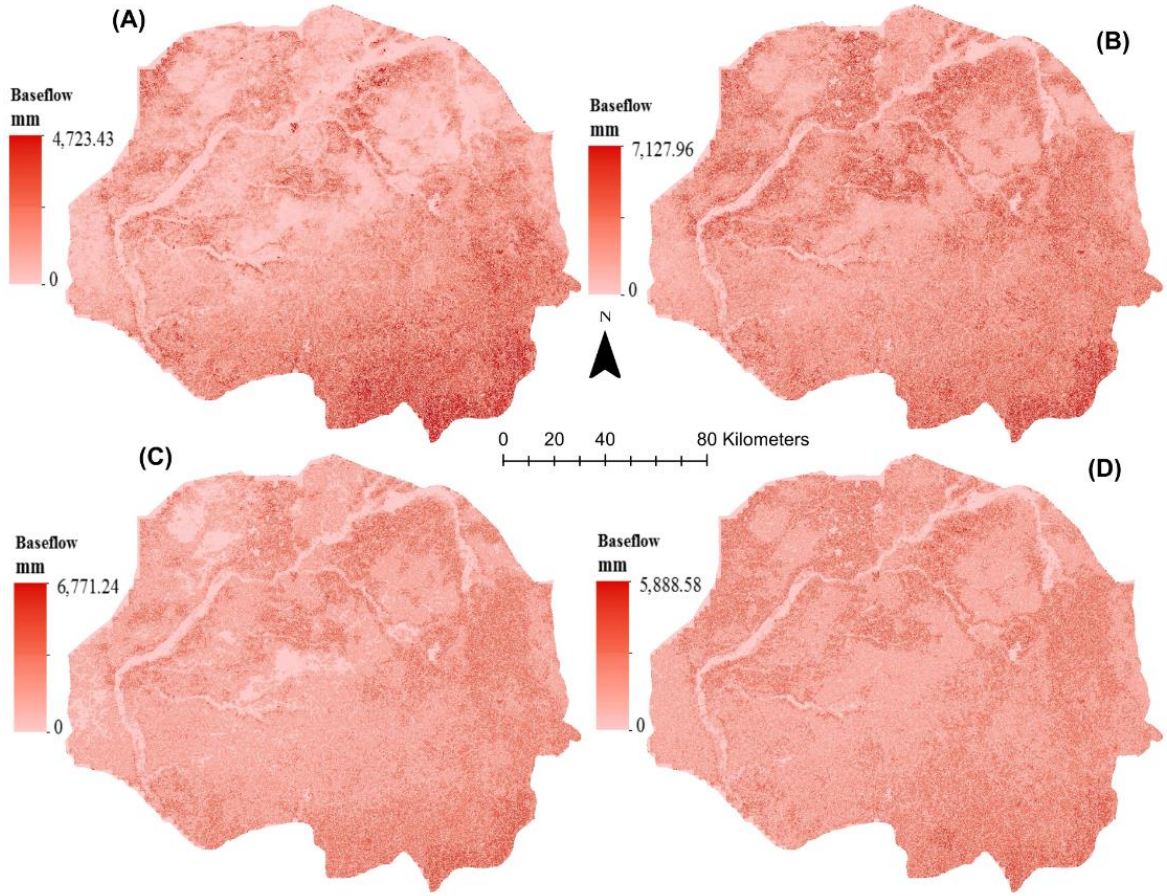

Figure 8 Dynamics of baseflow of the Sokoto Rima basin for the years 1992 (A), 2002 (B), 2012 (C) and 2015 (D)

There is some degree of spatial disparities in the pattern of baseflow of the Sokoto-Rima basin across this study. These observed variations are mapped and displayed in Figure 9, indicating non-linear dynamics in change patterns. The decade 1992-2002 showed that most of the study area recorded a mixed bag of dwindling and no-change pattern. There are exceptions of increase in wetland areas adjoining the major water bodies and woodlands where edaphic storage was detected to range between increase and zero variation. A completely different pattern was detected in the subsequent decade 2002-2012. An upsurge was noticed, obviously driven by cumulative precipitation input, with few exceptions in some of the north-western locations. The period 2012–2015 had minute decrease variations in some parts of the east and north while water bodies and floodplain of the Niger recorded no change. The aggregated spatial variation showed that a decrease in baseflow was detected in water bodies while the contiguous wetlands increased the quantum of baseflow.

Previous studies in the semi-arid areas of northern Nigeria, the nature and dynamics of groundwater characterization. [24] stated that the groundwater of the semi-arid northern Nigeria is generally available in small quantities, which to a considerable degree is the major source of potable water for its population. LR falls within the shallow groundwater, which is the main water point for the agricultural population of the Sokoto-Rima basin. Further, [24] opined that recharge from aquifer sources in the Sokoto-Rima basin is strongly influenced by geology. The Basement complex formation contributes an average of 40 mm/year, while others are affected by seasonal rainfall and proximity to water bodies ranged from 1 to 34 mm/year. However, it is anticipated that increasing demand for diverse water sources, majorly from municipal, agrarian, aquaculture and livestock coupled with climate change, sustainability of the current supply stock is vital. Thus projected that reliance on freshwater supplies from groundwater will increase by almost four-fold by 2030 [24-25].

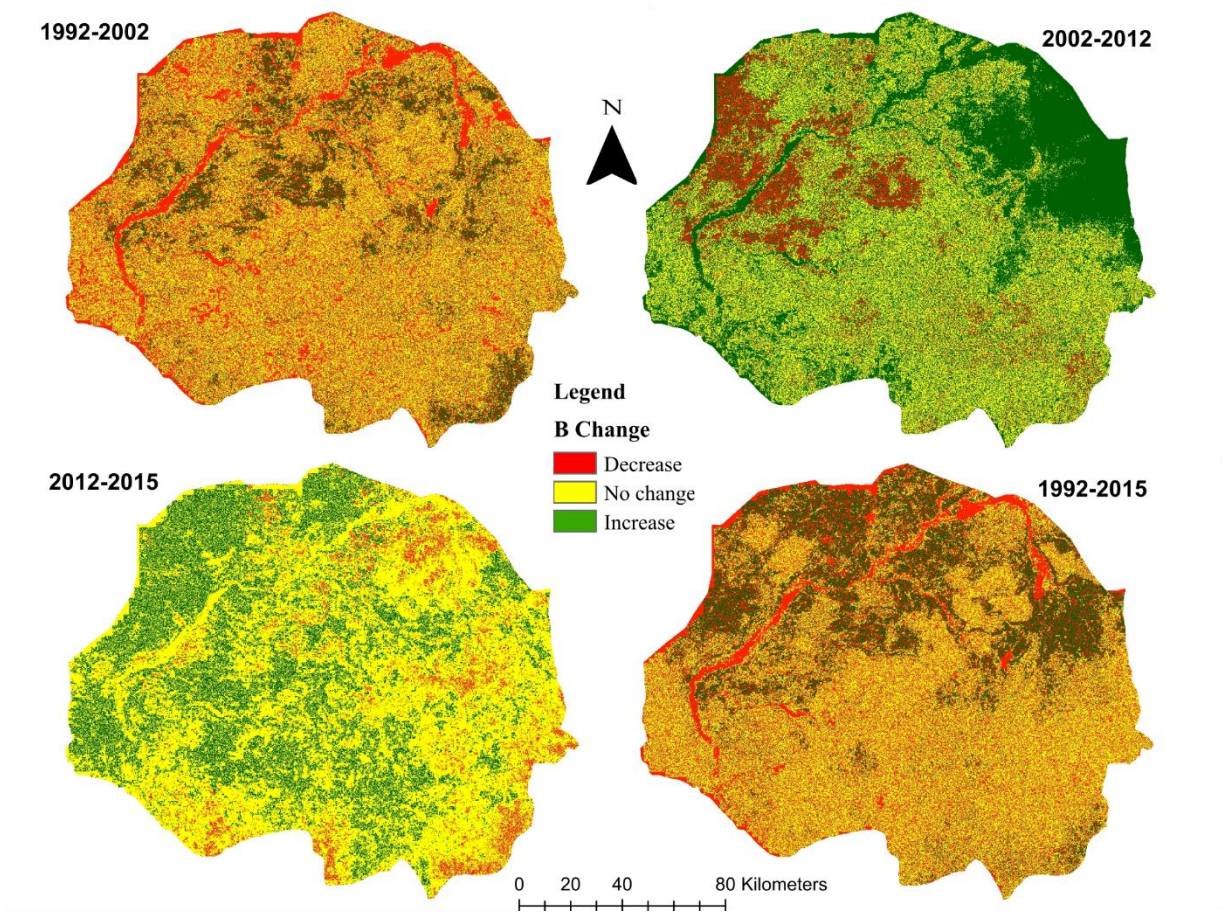

Figure 9 Pattern of spatiotemporal change in baseflow (B) in the Sokoto Rima basin for the period 1992 to 2015

3.4. Sensitivity Analysis of the SWY Model in the Sokoto-Rima basin

The set of equations used to typify the InVEST SWY model in terms of quickflow, local recharge, and baseflow are linear. Some of the associated variables nevertheless present a high possibility of sensitivity to changes in computational values. For instance, Figure 10 shows that a proportionate ±50% change in the critical parameters of θ, α, β, and γ can alter the amount of baseflow available per pixel within the multispectral space of the Sokoto-Rima basin. The least sensitive of the parameters assessed is f. Although this is analogous to the spatial resolution, it shows that threshold accumulation has a limited influence on baseflow. Thus, upslope relations and downslope reception exert limited influence on stream development. This is primarily related to the nature of the terrain as the Sokoto-Rima basin is geomorphologically a plain with exceptions along the eastern end where most of the rivers originate. The γ parameter returns some slight sensitivity with an average ±5.7% response to the proportionate adjustment. This sensitivity is a reflection of possible soil-water contexts under the influence of relief. This shows that soil-water relations are a local relief factor for baseflow availability annually. In addition, the soil characterisation contributes significantly to this extent of changes within the aquifer and groundwater traits possible within the semi-arid zone of Nigeria. The α and β parameters obviously influence baseflow as shown in Figure 10 with ±19% and ±15.7% response to adjustments, respectively. These are anticipated to drive increases and decreases in line with other covariates of water balance in the Sokoto-Rima basin and other similar semi-arid areas of West Africa. The shape and pattern of the response of these are also influenced to some degrees by landcover. For instance, [24] stated that baseflow characterisation is influenced by land characteristics, seasons and hydrogeological factors. α and β are direct correlates of these

factors integrated into the water balance computations enshrined into the InVEST SWY model. Local peculiarities are therefore critical in weighing the spatial performance of the InVEST SWY model.

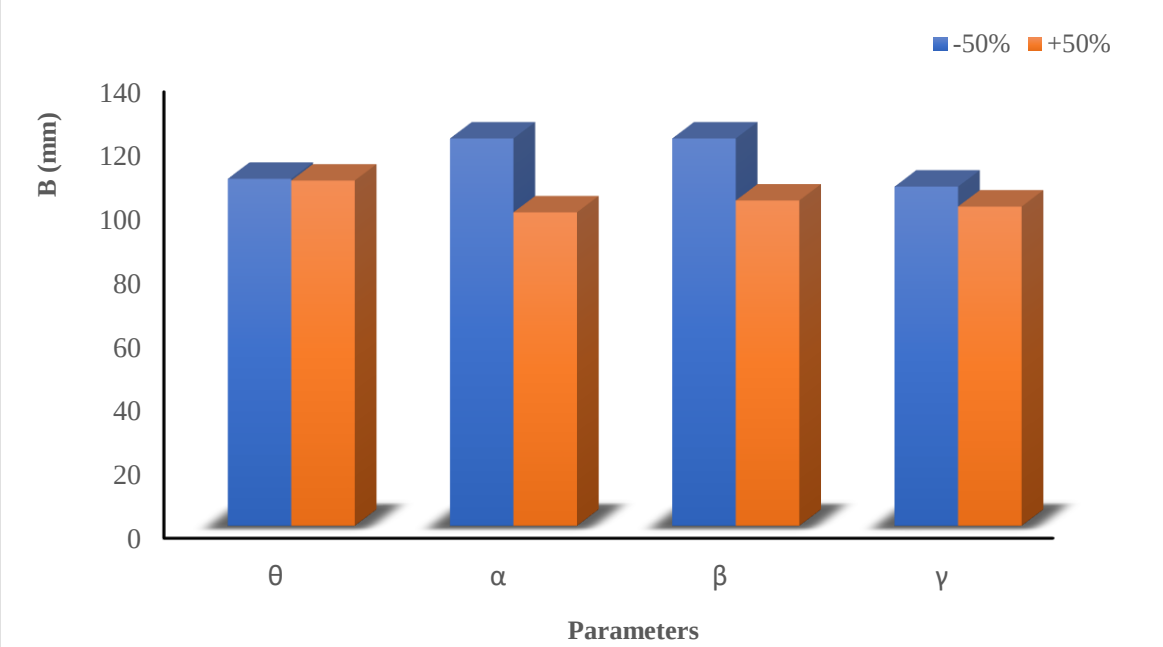

Figure 10 Pixel-based sensitivity test of the baseflow component of the SWY model as expressed by by f (Threshold accumulation), α (alpha parameter), β (beta parameter) and γ (gamma parameter)

3.5. Conclusion

Model-based computation of water yield using the tools of geographical information system is a burgeoning enterprise. In this research, we employed the SWY model in computing the quickflow, local recharge and baseflow using the InVEST software package for the semi-arid ecosystem of the northwestern part of Nigeria. The outcome mirrors some existing studies, particularly in terms of hydrogeological characteristics, seasonality and climate change on the computation of local recharge and baseflow, which are groundwater components of the study. This study becomes essential for the rational and deductive management of scarce water resources of the grasslands and savanna regions of the world where the Sokoto-Rima basin lies [26-27]. This will help policymakers use outputs of hydrological science as the basis for freshwater planning and management.

In addition, covariates of the adopted model require place-based sensitivity assessment to reflect data validation and model review areas. This has been tested for in the study, and the results showed that important covariates of baseflow exert significant influence on the aggregate quantity of SWY in the basin. Studies on landcover based scenarios on seasonal water yield on drylands such as the Sokoto-Rima basin help unveil context-specific factors influencing seasonal water yield and, to a large extent, the water balance relations.

4. REFERENCES

[1] Millennium Ecosystem Assessment, "Ecosystem and human well-being: biodiversity synthesis," 2005. Island Press, Washington DC.

[2] H. Saarikoski, E. Primmer, S. Saarela, P. Antunes, R. Aszalos, F. Baro, P. Berry, G. G. Blanko, E. Gomez-Baggethun, L. Carvalho, J. Dick, R. Dunford, M. Hanzu, P. A. Harrison, Z. Izakovicova, M. Kertész, L. Kopperoinen, B. Köhler, ... and J. Young, "Institutional challenges in putting ecosystem service knowledge in practice,"

Ecosystem Services, vol. 29, no. 3, pp. 579–598, 2018.

[3] J. Yang, Y. C. E. Yang, H. F. Khan, H. Xie, C. Ringler, A. Ogilvie, O. Seidou, A. G. Djibo, F. van Weert, and R. Therme, "Quantifying the sustainability of water availability for the water-food-energy-ecosystem nexus in the Niger River Basin," Earth's Future, vol 6, pp. 1292–1310, 2018.

[4] J. A. Aznar-Sánchez, J. F. Velasco-Muñoz, L. J. Belmonte-Ureña, and F. Manzano-Agugliaro, "The worldwide research trends on water ecosystem services," Ecological Indicators, vol. 99, pp. 310–323, 2019.

[5] C. Guo, and H. Xu, "Use of functional distinctness of periphytic ciliates for monitoring water quality in coastal ecosystems," Ecological Indicators, vol. 96, pp. 213–218, 2019.

[6] F. Scordo, T. Lavender, C. Seitz, V. Perillo, J. Rusak, M. Piccolo, and G. Perillo, "Modeling water yield: assessing the role of site and region-specific attributes in determining model performance of the InVEST seasonal water yield model", Water, vol. 10, pp. 1496, 2019.

[7] P. Hamel, J. Valencia, R. Schmitt, M. Shrestha, T. Piman, R. P. Sharp, W. Francesconi, and A. J. Gusawa, "Modeling seasonal water yield for landscape management: Applications in Peru and Myanmar. Journal of Environmental Management," Journal of Environmental Management, vol. 270, pp. 110792, 2020.

[8] I. J. Ekpoh, and E. Nsa, "The effects of recent climatic variations on water yield in the Sokoto region of northern Nigeria," International Journal of Business and Social Science, vol. 2, no. 7, pp. 251–256, 2011.

[9] S. A. Abdullahi, M. M. Muhammad, B. K. Adeogun, and I. U. Mohammed, "Assessment of water availability in the Sokoto Rima River Basin," Resources and Environment, vol. 4, no. 5, pp. 220–233, 2014.

[10] H. Hamidu, M. L. Garba, Y. I. Abubakar, U. Muhammad, and D. Mohammed, "Groundwater resource appraisals of Bodinga and environs, Sokoto Basin north western Nigeria," Nigerian Journal of Basic and Applied Science, vol. 24, no. 2, pp. 92–101, 2016.

[11] Food and Agriculture Organization of the United Nations, "FAO AQUASTAT: Country profile Nigeria," 2016. Available: http://www.fao.org/3/i9807en/I9807EN.pdf

[12] C. Albert, C. Galler, J. Hermes, F. Neuendorf, C. Von Haaren, A. Lovett, "Applying ecosystem services indicators in landscape planning and management: The ES-in-Planning framework," Ecological Indicators, vol. 61, pp., 100–113, 2016.

[13] J. C. Clanet and A. Ogilvie, "Basin focal project Niger," CPWF Project Report series, Challenge Program on Water and Food, Colombo, Sri Lanka, p 124.

[14] P. G. Oguntunde, B. J. Abiodun, and G. Lischeid, "Rainfall trends in Nigeria, 1901-2000", Journal of Hydrology, vol. 411, pp. 207–218, 2011.

[15] I. B. Abaje, O. F. Ati, and E. O. Iguisi, "Recent trends and fluctuations of annual rainfall in the sudano-sahelian ecological zone of Nigeria: Risks and opportunities," Journal of Sustainable Society, vol. 1, no. 2, pp. 44–51, 2012.

[16] G. B. Senay, S. Bohms, R. K. Singh, P. H. Gowda, N. M. Velpuri, H. Alemu, J. P. Verdin, "Operational evapotranspiration mapping using remote sensing and weather datasets: A new parameterization for the SSEB approach," Journal of American Water Resources Association, vol. 49, no. 3, pp. 577–591, 2013.

[17] R. I. Maidment, D. Grimes, E. Black, E. Tarnavsky, M. Young, H. Greatrex, R. P. Allan et al., "A new, long-term daily satellite-based rainfall dataset for operational monitoring in Africa," Nature Scientific Data, vol. 4, no. 170063, 2017. DOI:10.1038/sdata.2017.63.

[18] C. W. Ross, L. Prihodko, J. Anchang, S. Kumar, W. Ji, and N. P. Hanan, "HYSOGs250m, global gridded hydrologic soil groups for curve-number-based runoff modeling," Scientific Data, vol. 5, no. 180091. https://doi.org/10.1038/sdata.2018.91

[19] R. S. Sharp, H. T. Tallis, T. Ricketts, A. D. Guerry, S. A. Wood, E. Nelson, D. Ennaanay, S. Wolny, et al., "InVEST 3.7 User's Guide," 2019. Available: http://releases.naturalcapitalproject.org/invest-userguide/latest/

[20] S. U. Wali, K. J. Umar, S. D. Abubakar, I. P. Ifabiyi, I. M. Dankani, I. M. Shera, S. G. Yauri, "Hydrochemical characterization of shallow and deep groundwater in Basement Complex areas of southern Kebbi State, Sokoto Basin, Nigeria," Applied Water Science, vol. 9, no 169, 2019. https://doi.org/10.1007/s13201-019-1042-5

[21] Japan International Cooperation Agency, "The project for review and update of Nigeria national water resources master plan: Volume 5 Supporting report", Federal Ministry of Water Resources, Nigeria, 2014.

[22] S. M. A. Adelana, P. I. Olasehinde, and P. Vrbka, "Groundwater recharge in the cretaceous and tertiary sediment aquifers of northwestern Nigeria, using hydrochemical and isotopic techniques," Groundwater and Human Development, E. Bocanegra, D. Martínez, H. Massone, H (Eds.), pp. 907–915, 2002.

[23] S. M. A. Adelana, P. I. Olasehinde, R. B. Bale, P. Vrbka, A. G. Edet and I. B. Goni, "An overview of the geology and hydrogeology of Nigeria", in Applied groundwater studies in Africa, S. M. A. Adelana and A. M. McDonald, Eds. Leiden, Netherlands: CRC Press/Balkema, vol 13, pp. 171–198, 2008.

[24] S. M. A. Adelana, P. I. Olasehinde, and P. Vrbka, "A quantitative analysis of groundwater recharge in part of the Sokoto basin, Nigeria," Journal of Environmental Hydrology, vol. 14, no. 5, pp. 1–16, 2016.

[25] A. L. Vogl, J. H. Goldstein, G. C. Daily, B. Vira, L. L. Bremer, R. I. McDonald, D. Shemie, B. Tellman and J. Cassin, "Mainstreaming investments in watershed services to enhance water security: barriers and opportunities," Environmental Science and Policy, vol. 75, pp. 19–27, 2017. https://doi.org/10.1016/j.envsci.2017.05.007

[26] K. A. Brauman, "Hydrologic ecosystem services: linking ecohydrologic processes to human well-being in water research and watershed management." Wiley Interdiscip. Rev. Water, vol. 2, pp. 345–358, 2015. https://doi.org/10.1002/wat2.1081.

[27] C. E. R. Lehmann, "Savannas need protection". Science, vol. 327, pp. 642–643, 2010.

[28] A. J Guswa, P. Hamel, K. Meyer, "Curve number approach to estimate monthly and annual direct runoff," Journal of Hydrological Engineering, 23, 2018. https://doi.org/10.1061/(ASCE)HE.1943-5584.0001606.

[29] H. Lu, Y. Yan, J. Zhu, T. Jin, G. Liu, G. Wu, L. C. Stringer, M. Dallimer, "Spatiotemporal water yield variations and influencing factors in the Lhasa River Basin, Tibetan Plateau," Water, 12, 1498, 2020. doi:10.3390/w12051498

[30] S.Minga-León, M. A. Gómez-Albores, K. M. Bâ, L. Balcázar, L. R. Manzano-Solís, A. P. Cuervo-Robayo, C. A. Mastachi-Loza, "Estimation of water yield in the

hydrographic basins of southern Ecuador," Hydrology and Earth System Sciences, https://doi.org/10.5194/hess-2018-529

[31] K. Sang-Wook, and J. Yoon-Young, "Application of the InVEST model to quantify the water yield of North Korean forests," Forests, 11, 804, 2020. DOI:10.3390/f11080804.

[32] M. Sahle, O. Saito, C. Fürst, K. Yeshitela, "Quantifying and mapping of water-related ecosystem services for enhancing the security of the food-water-energy nexus in tropical data–sparse catchment," Science of The Total Environment, Vol 646, 573–586, 2019.

[33] X. Yang, R. Chen, M. E. Meadows, G. Ji, J. Xu, "Modelling water yield with the InVEST model in a data scarce region of northwest China," Water Supply. doi:10.2166/ws.2020.026

[34] United States Department of Agriculture (USDA) – Natural Resources Conservation Service (NRCS), Chapter 10: estimation of direct runoff from storm rainfall. In Part 630: Hydrology: NRCS National Engineering Handbook, USDA National Resources Conservation Service, 2004. https://directives.sc.egov.usda.gov/OpenNonWebContent.aspx?content=17752.wba